

Cite this: *Chem. Sci.*, 2018, **9**, 2552

## A chemiluminescent probe for cellular peroxynitrite using a self-immolative oxidative decarbonylation reaction†

Jian Cao,<sup>ab</sup> Weiwei An,<sup>ab</sup> Audrey G. Reeves<sup>a</sup> and Alexander R. Lippert  \*<sup>abc</sup>

Peroxynitrite ( $\text{ONOO}^-$ ) is a highly reactive oxygen species which has been recognized as an endogenous mediator of physiological activities like the immune response as well as a damaging agent of oxidative stress under pathological conditions. While its biological importance is becoming clearer, many of the details of its production and mechanism of action remain elusive due to the lack of available selective and sensitive detection methods. Herein, we report the development, characterization, and biological applications of a reaction-based chemiluminescent probe for  $\text{ONOO}^-$  detection, termed as PNCL. PNCL reacts with  $\text{ONOO}^-$  via an isatin moiety through an oxidative decarbonylation reaction to initiate light emission that can be observed instantly with high selectivity against other reactive sulphur, oxygen, and nitrogen species. Detailed studies were performed to study the reaction between isatin and  $\text{ONOO}^-$ , which confirm selectivity for  $\text{ONOO}^-$  over  $\text{NO}_2^\bullet$ . PNCL has been applied for  $\text{ONOO}^-$  detection in aqueous solution and live cells. Moreover, PNCL can be employed to detect cellular  $\text{ONOO}^-$  generated in macrophages stimulated to mount an immune response with lipopolysaccharide (LPS). The sensitivity granted by chemiluminescent detection together with the specificity of the oxidative decarbonylation reaction provides a useful tool to explore  $\text{ONOO}^-$  chemistry and biology.

Received 28th November 2017  
Accepted 31st January 2018

DOI: 10.1039/c7sc05087a  
[rsc.li/chemical-science](http://rsc.li/chemical-science)

## Introduction

Peroxynitrite ( $\text{ONOO}^-$ ) is a highly reactive oxygen species that can be formed biologically from a diffusion-controlled reaction between superoxide ( $\text{O}_2^-$ ) and nitric oxide ( $\text{NO}^\bullet$ ).<sup>1</sup> In biological systems,  $\text{ONOO}^-$  has long been known as a deleterious species due to its oxidative damage to lipids, proteins, and nucleic acids.<sup>2</sup> Abnormal regulation of  $\text{ONOO}^-$  in living systems is associated with diseases such as ischemia-reperfusion,<sup>3</sup> diabetes,<sup>4</sup> cardiac dysfunction,<sup>5</sup> inflammatory conditions,<sup>6</sup> autoimmune, and neurodegenerative diseases.<sup>7,8</sup> However,  $\text{ONOO}^-$  has been proposed to act as a physiological mediator in certain contexts, for example in immune system function<sup>9</sup> and ischemic preconditioning.<sup>10</sup> Macrophages produce nitric oxide and superoxide to form  $\text{ONOO}^-$  to attack invading pathogens.<sup>11</sup> Macrophage cells recognize lipopolysaccharide (LPS), a component of the bacterial cell wall, which induces high expression of inducible nitric oxide synthase (iNOS).<sup>12</sup> The effect of LPS is

amplified by release of IFN- $\beta$ , providing a mechanism for robust local production of  $\text{NO}^\bullet$  and  $\text{ONOO}^-$ . Although important biological functions of  $\text{ONOO}^-$  are still emerging, there remains a lack of efficient and selective methods to monitor its production in real time to study its effects in living systems. Therefore, the development of precise approaches for detecting  $\text{ONOO}^-$  is crucial to provide a more detailed understanding of its complex biological effects.

Much of the difficulty of studying the biological roles of  $\text{ONOO}^-$  stems from its complex chemistry.  $\text{ONOO}^-$  coexists with its protonated form  $\text{ONOOH}$  ( $\text{pK}_a$  6.8) under physiological pH, and can directly undergo two-electron reactions with thiols,<sup>13</sup>  $\text{CO}_2$ ,<sup>14</sup> and carbonyls.<sup>15</sup> The  $\text{H}^+$  and  $\text{CO}_2$  adducts,  $\text{ONOOH}$  and  $\text{ONOOOCO}_2^-$ , rapidly decompose *via* homolytic cleavage reactions to form secondary radicals such as hydroxyl radical ( $\text{HO}^\bullet$ ), carbonate radical ( $\text{CO}_3^{\cdot-}$ ), and nitrogen dioxide ( $\text{NO}_2^\bullet$ ), which mediate potent one-electron chemistry, including tyrosine nitration.<sup>16</sup>  $\text{ONOO}^-$  can also form from reaction between  $\text{O}_2$  and  $\text{NO}^\bullet$  produced by photolysis of Angeli's salt under alkaline conditions.<sup>17</sup> Under physiological conditions, Angeli's salt has been widely used as a nitroxyl (HNO) donor for biological studies. Reaction of HNO with  $\text{O}_2$  also proceeds at neutral pH to form a potent oxidative species and represents an important decomposition pathway of HNO.<sup>18,19</sup> While there are similarities and differences between  $\text{ONOO}^-$  and the autoxidation product of HNO formed at neutral pH, the details of this

<sup>a</sup>Department of Chemistry, Southern Methodist University, Dallas, TX 75275-0314, USA. E-mail: [alippert@smu.edu](mailto:alippert@smu.edu)

<sup>b</sup>Center for Drug Discovery, Design, and Delivery (CD4), Southern Methodist University, Dallas, TX 75275-0314, USA

<sup>c</sup>Center for Global Health Impact (CGHI), Southern Methodist University, Dallas, TX 75275-0314, USA

† Electronic supplementary information (ESI) available: Additional experimental details, supplementary figures, and scanned spectra. See DOI: [10.1039/c7sc05087a](https://doi.org/10.1039/c7sc05087a)



chemistry and the exact species eliciting the oxidative effect of Angeli's salt is still under debate.

The classical approach for studying biological  $\text{ONOO}^-$  relies on immunostaining of 3-nitrotyrosine residues,<sup>20</sup> which lacks temporal precision and is an indirect method tracking the "footprint" of  $\text{ONOO}^-$ . A large number of reaction-based fluorescent probes have been developed in an attempt to solve this problem. These small molecule tools can react with chemical species as they are produced, enabling detection within living intact systems. Several families of reaction-based fluorescent probes for  $\text{ONOO}^-$  detection have been reported and applied in biological studies, such as trifluorocarbonyl-based,<sup>21</sup> *N*-dearylation-based,<sup>22</sup> and boronic ester-based<sup>23</sup> probes. Organoselenium-based,<sup>24</sup> and organotellurium-based<sup>25</sup> probes are advantageous because the fluorescence signal is reversible, but depend upon reaction with cellular reductants to reverse the signal.<sup>26</sup> This limited reversibility, as well as other intrinsic drawbacks of fluorescent detection methods such as photo-bleaching and autofluorescence highlights the need for new methods of  $\text{ONOO}^-$  detection. Chemiluminescence provides an attractive solution for studying biological molecules and processes due to the low background, high signal-to-noise ratio, and reversible signal of this technique.<sup>27</sup> Nanoparticle-based methods have recently been reported for chemiluminescent  $\text{ONOO}^-$  detection.<sup>28,29</sup> These probes rely on an interesting radical-pair mechanism to generate signal from the  $\text{ONOO}^-$  decomposition products  $\text{HO}^\cdot$  and  $\text{O}_2^-$ . Although these systems do display good sensitivity, complementary approaches that operate *via* direct reaction with  $\text{ONOO}^-$  are desirable. Chemiluminescent probes based on sterically hindered 1,2-dioxetanes offer opportunities to incorporate specific reaction-based triggers and have already been applied for detection of analytes in cellular systems and for live animal imaging.<sup>30-34</sup> One fruitful design strategy uses Schaap's adamantylidene-dioxetane attached to an analyte-specific reactive handle.<sup>35</sup> A striking substituent effect for Schaap's 1,2-dioxetanes has been reported, where incorporation of an electron withdrawing group such as an acrylonitrile at the *ortho* position of the phenol results in a significant increase in the overall chemiluminescent quantum yield of 1,2-dioxetanes.<sup>36</sup> As a result, chemiluminescent emission can be observed in aqueous conditions without the addition of any polymeric enhancer solutions. We herein describe the development and application of a selective chemiluminescent probe for  $\text{ONOO}^-$  detection, **PNCL**, with both *in vitro* and live cell applications.

## Results and discussion

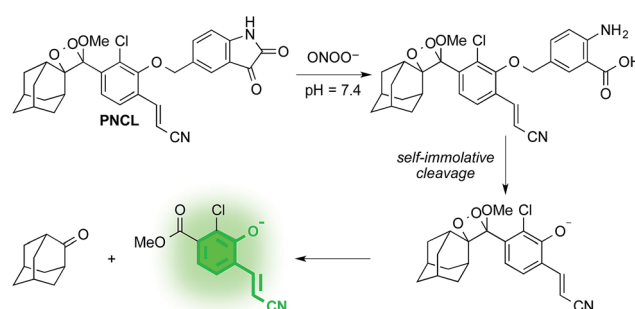
### Design and synthesis of **PNCL**

As part of a program to develop chemical probes for imaging reactive sulphur,<sup>29,37</sup> oxygen,<sup>30,38,39</sup> and nitrogen species, our laboratory has previously reported that isatin reacts with  $\text{ONOO}^-$  *via* an oxidative decarbonylation reaction to generate anthranilic acid.<sup>40</sup> <sup>19</sup>F NMR probes, 5-fluoroisatin and 6-fluorisatin, have been developed for selective detection of  $\text{ONOO}^-$  that utilize this newly discovered transformation. In order to expand this reaction-based detection strategy for luminogenic

detection, we adopted a self-immolative 1,6-elimination strategy for chemiluminescent  $\text{ONOO}^-$  detection that relies on tethering an isatin moiety to a 1,2-dioxetane chemiluminescent scaffold *via* an ether linkage (Scheme 1). The isatin serves as the reaction handle, and 1,6-elimination can be triggered after reacting with  $\text{ONOO}^-$  to form the anthranilic acid with the amino group positioned *para* to the benzylic ether. Luminescent emission is then initiated upon the decomposition of the 1,2-dioxetane through a chemically initiated electron exchange luminescence (CIEL) mechanism. Synthesis of a peroxynitrite chemiluminescent probe (**PNCL**) proceeded from commercially available 5-iodoisatin **1** by protection of the ketone group as the dimethylacetal **2** (Scheme 2). The protected 5-iodoisatin was subjected to palladium catalyzed reductive formylation with *N*-formyl saccharin as the CO source to form the aldehyde **3**,<sup>41</sup> followed by reduction of the aldehyde with  $\text{NaBH}_4$  and deprotection to afford benzyl alcohol **4**. The alcohol **4** was linked to the phenol **5** (ref. 36) through a Mitsunobu reaction to deliver the enol ether precursor **6**. This precursor underwent [2 + 2] cycloaddition with photogenerated singlet oxygen using Rose Bengal as a sensitizer to provide the final 1,2-dioxetane **PNCL**.

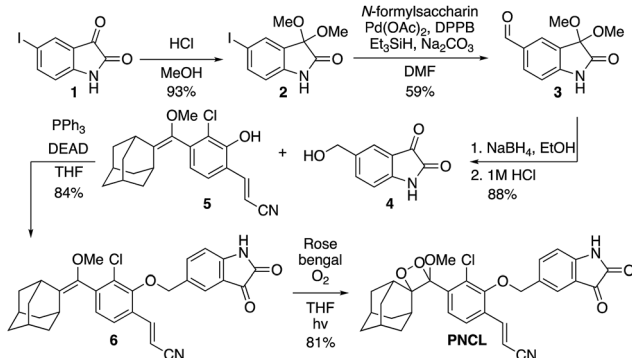
### Spectral response of the probes to $\text{ONOO}^-$

After obtaining **PNCL**, its photophysical properties and reactivity towards  $\text{ONOO}^-$  were characterized. Luminescence emission spectra were collected using an F-7000 Hitachi spectrophotometer by treating 20  $\mu\text{M}$  **PNCL** with 0–200  $\mu\text{M}$   $\text{ONOO}^-$  (Fig. 1). An emission peak centered at 525 nm was observed in the presence of  $\text{ONOO}^-$  with  $\sim$ 28-fold increase in peak luminescence intensity compared to a blank control (Fig. 1A). The reaction between **PNCL** and  $\text{ONOO}^-$  was analyzed by GC-MS, confirming the generation of 2-adamantanone and 2-chloro-4-acrylonitrile-3-(methoxycarbonyl)phenol (Fig. S1†). The luminescence emission slowly decayed over a course of 20 min (Fig. 1B), consistent with fast reaction kinetics of  $\text{ONOO}^-$  with the isatin moiety of **PNCL**,<sup>40</sup> followed by a slower 1,6-elimination. Interestingly,  $\text{ONOO}^-$  can be added to a solution of **PNCL** over several cycles with good recovery of chemiluminescent signal (Fig. S2†). This shows that the reversible chemiluminescent emission has good reproducibility and can be used to monitor  $\text{ONOO}^-$  fluxes over time. The dose dependence of the peak chemiluminescent emission at 525 nm measured 10



Scheme 1 Spiroadamantane 1,2-dioxetane-based probe for chemiluminescent  $\text{ONOO}^-$  detection.





Scheme 2 Synthesis of PNCL.

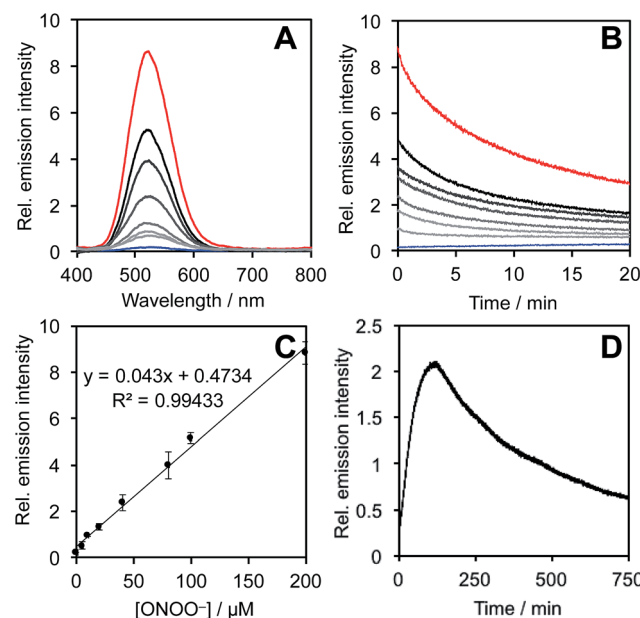


Fig. 1 Response of PNCL to  $\text{ONOO}^-$ . (A) Chemiluminescent emission spectra of 20  $\mu\text{M}$  PNCL and 0 (blue trace), 5, 10, 20, 40, 80, 100, 200  $\mu\text{M}$  (red trace)  $\text{ONOO}^-$ . (B) Time scans of the chemiluminescent emission at 525 nm of 20  $\mu\text{M}$  PNCL and 0 (blue trace), 5, 10, 20, 40, 80, 100, 200  $\mu\text{M}$  (red trace)  $\text{ONOO}^-$ . (C) Peak emission intensity at 525 nm of 20  $\mu\text{M}$  PNCL after adding 0–200  $\mu\text{M}$   $\text{ONOO}^-$ . (D) Time scan of the chemiluminescent emission at 525 nm of 20  $\mu\text{M}$  PNCL and 200  $\mu\text{M}$  SIN-1. All experiments were performed in 20 mM HEPES (pH 7.4), containing <1% DMSO.

seconds after  $\text{ONOO}^-$  addition showed excellent linearity, demonstrating that  $\text{ONOO}^-$  can be quantified using PNCL (Fig. 1C). Calibration of the response of PNCL with lower concentrations of  $\text{ONOO}^-$  revealed a detection limit of 6 nM ( $3\sigma$ ) bolus  $\text{ONOO}^-$  (Fig. S3†), comparing favorably to previous fluorescent and chemiluminescent methods (Table S1†). The reactivity of PNCL towards SIN-1 was also evaluated (Fig. 1D), showing that PNCL can monitor the slow release of  $\text{ONOO}^-$  over time, as would be observed in biological systems.

The selectivity of PNCL for  $\text{ONOO}^-$  was tested against a panel of biologically relevant reactive sulphur, oxygen, and nitrogen species and metal cations. The response of PNCL to

200  $\mu\text{M}$   $\text{ONOO}^-$  was compared against other analytes in HEPES buffer (20 mM, pH 7.4), by adding 5 mM reduced glutathione (GSH), 1 mM L-cysteine, or 200  $\mu\text{M}$  other reactive species. Most of the species tested displayed no significant increase in luminescence intensity over the blank control within 20 min (Fig. 2). Given the destructive reactivity of  $\text{HO}^\cdot$ , we examined the interference of this species by treating PNCL with  $\text{ONOO}^-$  in the presence of the  $\text{HO}^\cdot$ -generating Fenton system (Fig. S4†), where only a minimal reduction in signal was observed. A small luminescence increase was observed when treating PNCL with Angeli's salt, commonly used as a nitroxyl ( $\text{HNO}$ ) donor. This was consistent with previous observations using HPLC to track the reactivity of 5-fluoroisatin with Angeli's salt.<sup>37</sup>

In light of studies exploring the generation of  $\text{ONOO}^-$  and other nitrogen oxide species from the autoxidation of  $\text{NO}^-$  and  $\text{HNO}$ ,<sup>17–19</sup> we performed a series of competition experiments with  $\text{HCO}_3^-$  and GSH to better understand the luminescence increase resulting from reaction of PNCL with Angeli's salt.  $\text{ONOO}^-$  reacts rapidly with  $\text{CO}_2$ , but slowly with GSH.  $\text{HNO}$ , on the other hand, reacts rapidly with GSH.<sup>42</sup> We treated PNCL with  $\text{ONOO}^-$  (Fig. 3A and B) or Angeli's salt (Fig. 3C and D) in the presence of various amount of  $\text{HCO}_3^-$  (1 mM, 2 mM, 3 mM, 4 mM, and 5 mM).  $\text{HCO}_3^-$  decreased the chemiluminescence emission intensity generated by both  $\text{ONOO}^-$  and Angeli's salt, providing evidence that Angeli's salt can generate  $\text{ONOO}^\cdot$ . A similar experiment was performed by reacting PNCL (20  $\mu\text{M}$ ) with  $\text{ONOO}^-$  (Fig. 4A and B) or Angeli's salt (Fig. 4C and D) and various amounts of GSH (50  $\mu\text{M}$ , 100  $\mu\text{M}$ , 200  $\mu\text{M}$ , and 1 mM). However, the GSH only quenched the luminescence intensity from Angeli's salt (Fig. 4B) and no significant luminescence decrease was observed from  $\text{ONOO}^-$  (Fig. 4A). Interestingly, substoichiometric quantities of GSH would not only reduce the total amount of luminescence, but displayed a lag time before producing a chemiluminescent signal (Fig. 4C). Angeli's salt generates  $\text{HNO}$  with a half-life of 2.3 minutes at 37 °C. The observed lag time of the chemiluminescent response is

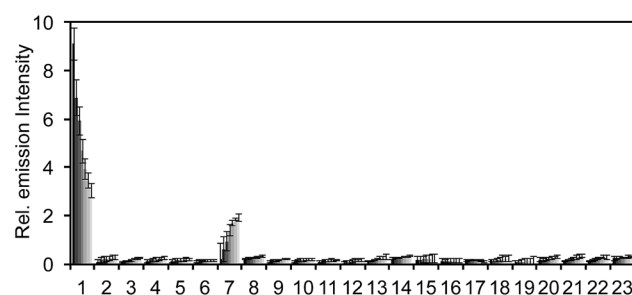


Fig. 2 Selectivity of PNCL versus cations and reactive sulphur, oxygen, and nitrogen species. Chemiluminescent emission at 525 nm of 20  $\mu\text{M}$  PNCL and 200  $\mu\text{M}$  biologically relevant analytes in 20 mM HEPES (pH 7.4). Bars represent chemiluminescent emission at 525 nm at 4, 8, 12, 16, 20 min after addition of reactive species. Legend: (1)  $\text{ONOO}^-$ , (2) Cys, (3) DEA NONOate, (4) GSH (5 mM), (5) GSNO, (6)  $\text{H}_2\text{O}_2$ , (7) Angeli's salt, (8)  $\text{KO}_2$ , (9)  $\text{Na}_2\text{S}$ , (10)  $\text{Na}_2\text{S}_2\text{O}_3$ , (11)  $\text{Na}_2\text{SO}_4$ , (12)  $\text{NaNO}_2$ , (13)  $\text{HO}^\cdot$ , (14)  $\text{OCl}^-$ , (15)  $\text{tBuOOH}$ , (16)  ${}^1\text{O}_2$ , (17)  $\text{Na}^+$ , (18)  $\text{Mg}^{2+}$ , (19)  $\text{K}^+$ , (20)  $\text{Ca}^{2+}$ , (21)  $\text{Zn}^{2+}$ , (22)  $\text{Fe}^{2+}$ , (23) blank. Error bars are  $\pm$  S.D. All experiments were performed in 20 mM HEPES or 20 mM PBS (pH 7.4), containing <1% DMSO.



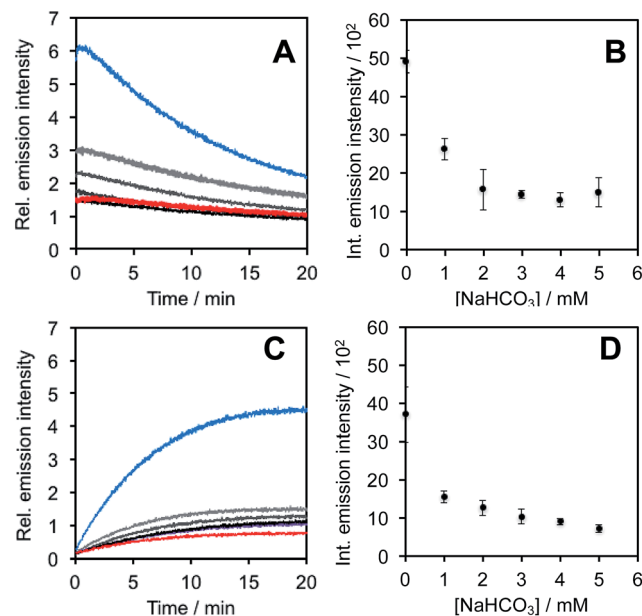


Fig. 3 Inhibition of response by  $\text{NaHCO}_3$ . (A) Time scans and (B) integrated intensity of the chemiluminescent emission of  $20 \mu\text{M}$  PNCL,  $200 \mu\text{M}$   $\text{ONOO}^-$  and 0 (blue trace),  $1 \text{ mM}$ ,  $2 \text{ mM}$ ,  $3 \text{ mM}$ ,  $4 \text{ mM}$ , and  $5 \text{ mM}$  (red trace)  $\text{NaHCO}_3$ . (C) Time scans and (D) integrated intensity of the chemiluminescent emission of  $20 \mu\text{M}$  PNCL,  $200 \mu\text{M}$  Angeli's salt and 0 (blue trace),  $1 \text{ mM}$ ,  $2 \text{ mM}$ ,  $3 \text{ mM}$ ,  $4 \text{ mM}$ , and  $5 \text{ mM}$  (red trace)  $\text{NaHCO}_3$ . All experiments were performed in  $20 \text{ mM}$  HEPES (pH 7.4), containing <1% DMSO.

consistent with GSH scavenging the newly formed HNO more rapidly than the autoxidation reaction of HNO. Once the GSH is consumed, HNO can be oxidized to  $\text{ONOO}^-$  or another nitrogen oxide species capable of two-electron chemistry and reaction with PNCL proceeds to produce a luminescent signal.

In order to confirm this selectivity and that  $\text{HCO}_3^-/\text{CO}_2$  does not scavenge HNO, we prepared a fluorescent nitroxyl (HNO) probe, herein called **XF1** (Fig. 5A). HNO reacts with the diphenylphosphinobenzoyl group to form an aza-ylide that will nucleophilically attack the ester to trigger the release of the fluorophore.<sup>43,44</sup> A time-dependent fluorescence turn-on was observed when treating  $10 \mu\text{M}$  **XF1** with  $200 \mu\text{M}$  Angeli's salt (Fig. S5A and B†), and selectivity tests demonstrated that **XF1** can distinguish HNO from other reactive sulfur, oxygen, and nitrogen species (Fig. S5C†). Inhibition experiments were conducted by treating **XF1** with various amounts of  $\text{HCO}_3^-$  or GSH together with Angeli's salt. While no obvious inhibition of the fluorescence response was observed with the addition of  $\text{HCO}_3^-$ , the fluorescence was completely quenched with  $200 \mu\text{M}$  GSH (Fig. 5B and C). These results confirm that GSH scavenges HNO generated from Angeli's salt but  $\text{HCO}_3^-/\text{CO}_2$  does not scavenge HNO. Taken together, the results from Fig. 3–5 are consistent with the luminescence increase from Angeli's salt being due to the generation of  $\text{ONOO}^-$ . We do note that alternative oxidative species formed from HNO have been proposed.<sup>18</sup> Although we cannot completely rule this out, the results here are consistent with the formation of  $\text{ONOO}^-$  from HNO and support the high specificity of PNCL for detecting

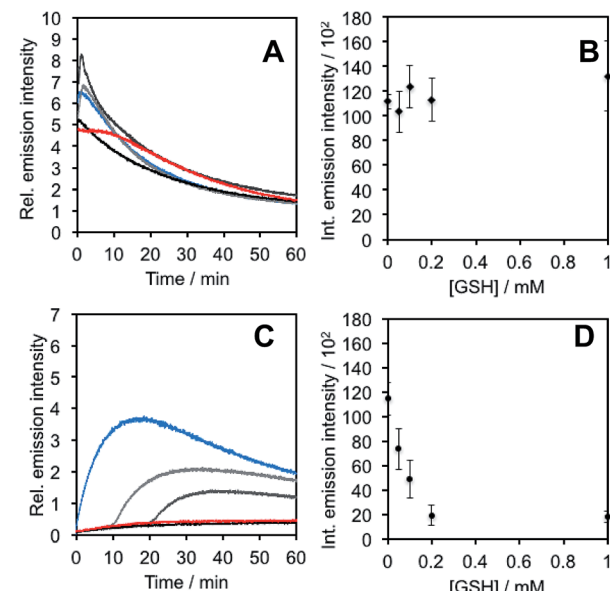


Fig. 4 Inhibition of response by glutathione. (A) Time scans and (B) integrated intensity of the chemiluminescent emission of  $20 \mu\text{M}$  PNCL,  $200 \mu\text{M}$   $\text{ONOO}^-$  and 0 (blue trace),  $50 \mu\text{M}$ ,  $100 \mu\text{M}$ ,  $200 \mu\text{M}$ , and  $1 \text{ mM}$  (red trace) glutathione. (C) Time scans and (D) integrated intensity of the chemiluminescent emission of  $20 \mu\text{M}$  PNCL,  $200 \mu\text{M}$  Angeli's salt and 0 (blue trace),  $50 \mu\text{M}$ ,  $100 \mu\text{M}$ ,  $200 \mu\text{M}$ , and  $1 \text{ mM}$  (red trace) glutathione. All experiments were performed in  $20 \text{ mM}$  HEPES (pH 7.4), containing <1% DMSO.

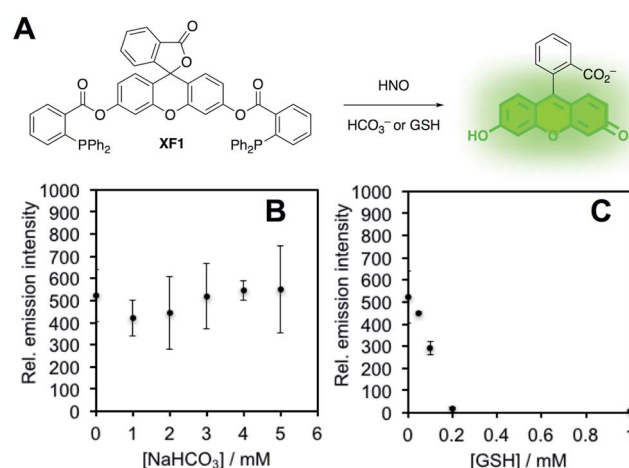


Fig. 5 HNO scavenging by  $\text{NaHCO}_3$  and GSH. (A) Design of **XF1**, a fluorescent probe for HNO. (B) Peak emission intensity of  $10 \mu\text{M}$  **XF1**,  $200 \mu\text{M}$  Angeli's salt and  $0$ – $5 \text{ mM}$   $\text{NaHCO}_3$ . (C) Peak emission intensity of  $10 \mu\text{M}$  **XF1**,  $200 \mu\text{M}$  Angeli's salt and  $0$ – $1 \text{ mM}$  glutathione. All experiments were performed in  $20 \text{ mM}$  HEPES (pH 7.4), containing <1% DMSO with  $\lambda_{\text{ex}} = 488 \text{ nm}$ .

$\text{ONOO}^-$ . As a final mechanistic investigation, we examined the selectivity of  $\text{ONOO}^-$  versus  $\text{NO}_2^\cdot$ ,  $\text{HO}^\cdot$ , and  $\text{CO}_3^{2-}$  (the decomposition products of  $\text{ONOO}^-$ ) by treating isatin with  $\text{ONOO}^-$  in the presence of  $\text{HCO}_3^-/\text{CO}_2$  or TEMPOL, a free radical scavenger (Fig. S6†). While  $\text{HCO}_3^-/\text{CO}_2$  inhibits the reaction, TEMPOL has no effect. This suggests that isatin reacts directly with  $\text{ONOO}^-$ .

and not with free radical species like  $\text{NO}_2^\cdot$ ,  $\text{HO}^\cdot$ , or  $\text{CO}_3^{\cdot-}$  that are formed *via* spontaneous  $\text{ONOO}^-$  decomposition.

### Evaluation of PNCL for $\text{ONOO}^-$ detection in living cells

After demonstrating that PNCL reacts with  $\text{ONOO}^-$  with high sensitivity and selectivity, we then proceeded to investigate the ability of PNCL for  $\text{ONOO}^-$  detection in living cells using a BioTek Cytation 5 plate reader. Toxicity was determined by the MTT assay, which indicated low toxicity after 24 hour treatment with PNCL at concentrations less than 100  $\mu\text{M}$  and more than 50% viability after treating with high concentrations of 1 mM PNCL for 24 hours (Fig. S7†). Cellular internalization was verified by imaging the intrinsic fluorescence emission of PNCL (Fig. S8†). In order to evaluate the ability of PNCL to detect cellular delivery of  $\text{ONOO}^-$  from donor compounds, RAW 264.7 macrophages were incubated with PNCL for 30 minutes, washed, and then treated with 0, 200  $\mu\text{M}$ , 400  $\mu\text{M}$ , 800  $\mu\text{M}$ , 1 mM, or 2 mM SIN-1, a commonly used  $\text{ONOO}^-$  donor that operates by simultaneously generating  $\text{NO}^\cdot$  and  $\text{O}_2^{\cdot-}$ . A time course of the chemiluminescent emission intensity increased to reach a maximum at 40 minutes (Fig. 6A). Both the peak and integrated luminescence intensities increased with increasing concentrations of SIN-1 (Fig. 6A and B), and a 5-fold luminescence increase was obtained with 2 mM SIN-1 compared with

a blank control. We also performed the same experiment in A549 cells (Fig. S9†). Similar results were observed and excellent linearity was achieved in living cells between 0 and 400  $\mu\text{M}$  SIN-1 (Fig. S9C†). This increase in chemiluminescent emission from SIN-1 and PNCL was attenuated by the  $\text{ONOO}^-$  scavenger Mn(III)TMPyP (Fig. S10†), confirming that the response is due to  $\text{ONOO}^-$ .

Finally, we investigated the ability of PNCL to detect  $\text{ONOO}^-$  generated by macrophages stimulated to mount an immune response. Lipopolysaccharide (LPS) binds to the toll-like receptors of macrophages, activating the transcription factor  $\text{NF-}\kappa\beta$  ultimately leading to the expression of iNOS and generation of reactive oxygen species that can produce  $\text{ONOO}^-$ .<sup>12</sup> Macrophages stimulated with LPS produced increased chemiluminescent signal from PNCL (Fig. 6C), showing a 36% increase in integrated luminescence intensity with 1000 ng  $\text{mL}^{-1}$  LPS. Treatment with the  $\text{ONOO}^-$  scavenger Mn(III)TMPyP reduces this signal back to control levels and co-incubation with the selective iNOS inhibitor 1400 W also reduces the signal from LPS and PNCL (Fig. S11†). These control experiments validate the ability of PNCL to detect cellular production of  $\text{ONOO}^-$ . Bright field images of the cells after LPS stimulation show the formation of phagosomes (Fig. 6D), a phenotypic response to LPS exposure.

## Conclusions

We have designed and synthesized a reaction-based chemiluminescent probe for  $\text{ONOO}^-$ , PNCL. PNCL reacts with  $\text{ONOO}^-$  through an oxidative decarbonylation reaction to initiate light emission that can be observed instantly with high sensitivity and selectivity against other reactive sulphur, oxygen, and nitrogen species. The observed reactivity towards Angeli's salt is attributed to the generation of  $\text{ONOO}^-$ , which is supported by inhibitor experiments with  $\text{HCO}_3^-$  and GSH, providing experimental evidence of an autoxidative product of HNO. Several studies have purported that the autoxidation of HNO produces a product unique from  $\text{ONOO}^-$ , as evidenced by data showing no effect of  $\text{HCO}_3^-$  on the reaction between Angeli's salt and reactive oxygen species probe dihydrorhodamine 123.<sup>18</sup> In our studies, however, we observe a drastic  $\text{HCO}_3^-$  dependent reduction in chemiluminescent signal from PNCL and Angeli's salt, consistent with  $\text{ONOO}^-$  formation from HNO under physiological conditions.<sup>19</sup> PNCL was used to detect  $\text{ONOO}^-$  generated from donor compounds in multiple cell lines, as well as cellular  $\text{ONOO}^-$  generated by macrophages stimulated with LPS. Confirmation of the chemical specificity towards  $\text{ONOO}^-$  over downstream free radical products, coupled with operational compatibility in living cells establishes PNCL a useful and easy-to-use tool for studying  $\text{ONOO}^-$  in chemical and biological systems.

## Conflicts of interest

A. R. L. discloses a financial stake in BioLum Science, LLC, a company developing asthma monitoring technology.

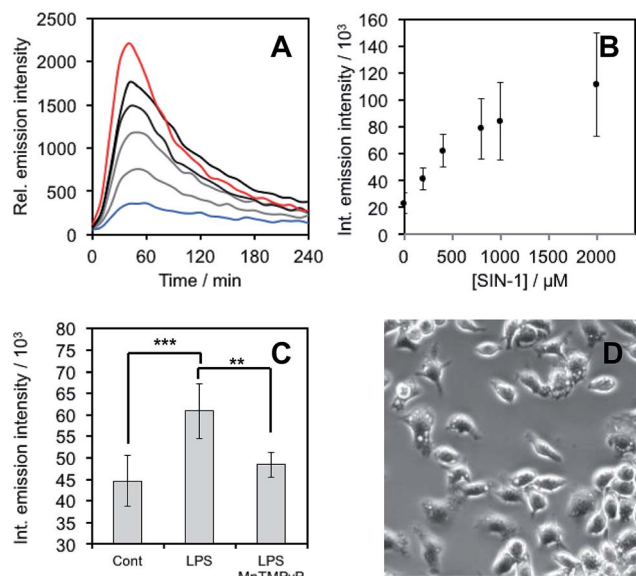


Fig. 6  $\text{ONOO}^-$  detection in RAW 264.7 macrophages. (A) Time scans and (B) integrated intensity of chemiluminescence emission of RAW 264.7 macrophages incubated with 20  $\mu\text{M}$  PNCL for 30 minutes, washed, and then treated with 0 (blue trace), 200  $\mu\text{M}$ , 400  $\mu\text{M}$ , 800  $\mu\text{M}$ , 1 mM, and 2 mM SIN-1, a commonly used  $\text{ONOO}^-$  donor that operates by simultaneously generating  $\text{NO}^\cdot$  and  $\text{O}_2^{\cdot-}$ . (C) Integrated chemiluminescent emission intensity of RAW 264.7 macrophages stimulated with (Cont) Vehicle control, (LPS) 1000 ng  $\text{mL}^{-1}$  LPS, or (LPS, MnTMPyP) 1000 ng  $\text{mL}^{-1}$  LPS and 25  $\mu\text{M}$  Mn(III)TMPyP and then treated with 20  $\mu\text{M}$  PNCL. (D) Brightfield images of stimulated RAW 264.7 macrophages. Error bars are S.D. from  $n = 3\text{--}7$  wells and 3 biological replicates ( $n = 10$  wells from 6 biological replicates for the control experiment). Statistical significance was assessed using a two-tailed student's  $t$ -test. \*\*\* $p < 0.001$ , \*\* $p < 0.01$ .



## Acknowledgements

Research reported in this publication was supported by the National Institute Of General Medical Sciences of the National Institutes of Health under award number R15GM114792. The content is solely the responsibility of the authors and does not necessarily represent the official views of the National Institutes of Health. Additional support was provided by Southern Methodist University (start-up funds to A. R. L and Engaged Learning funds to A. G. R.). We acknowledge Manasa Subbarao for assistance with cell culture and Sara Lange for assistance with preliminary experiments. We thank Maciej Kukula (UT Arlington), Hamilton Lee (UT Dallas), and Prof. Jeremiah Gassensmith (UT Dallas) for assistance with mass spectrometry. Human lung adenocarcinoma epithelial cell (A549) were purchased from ATCC and cultured in F-12K media supplemented with 10% Fetal Bovine Serum (FBS) and 1% antibiotics (penicillin/streptomycin, 100 U mL<sup>-1</sup>).

## Notes and references

- 1 J. S. Beckman, T. W. Beckman, J. Chen, P. A. Marshall and B. A. Freeman, *Proc. Natl. Acad. Sci. U. S. A.*, 1990, **87**, 1620.
- 2 (a) A. J. Gow, D. Duran, S. Malcolm and H. Ischiropoulos, *FEBS Lett.*, 1996, **385**, 63; (b) G. L. Squadrito and W. A. Pryor, *Free Radical Biol. Med.*, 1998, **25**, 392; (c) C. Szabó, H. Ischiropoulos and R. Radi, *Nat. Rev. Drug Discovery*, 2007, **6**, 662; (d) P. Pacher, J. S. Beckman and L. Liaudet, *Physiol. Rev.*, 2007, **87**, 315.
- 3 P. Liu, B. H. Xu, J. Quilley and P. Y. K. Wong, *Am. J. Physiol.: Cell Physiol.*, 2000, **279**, 1970.
- 4 W. Kossenjans, A. Eis, R. Sahay, D. Brockman and L. Myatt, *Am. J. Physiol.: Heart Circ. Physiol.*, 2000, **278**, 1311.
- 5 P. B. Massion, O. Feron, C. Dessy and J. L. Balligand, *Circ. Res.*, 2003, **93**, 388.
- 6 H. Wiseman and B. Halliwell, *Biochem. J.*, 1996, **313**, 17.
- 7 R. Ahmad, Z. Rasheed and H. Ahsan, *Immunopharmacol. Immunotoxicol.*, 2009, **31**, 388.
- 8 (a) J. S. Beckman, M. Carson, C. D. Smith and W. H. Koppenol, *Nature*, 1993, **364**, 584; (b) M. A. Smith, P. L. R. Harris, L. M. Sayre, J. S. Beckman and G. Perry, *J. Neurosci.*, 1997, **17**, 2653; (c) N. A. Simonian and J. T. Coyle, *Annu. Rev. Pharmacol. Toxicol.*, 1996, **36**, 83.
- 9 C. Brito, M. Naviliat, A. C. Tiscornia, F. Vuillier, G. Gualco, G. Dighiero, R. Radi and A. M. Cayota, *J. Immunol.*, 1999, **162**, 3356–3366.
- 10 S. Altug, A. T. Demiryürek, K. A. Kane and I. Kanzik, *Br. J. Pharmacol.*, 2000, **130**, 125.
- 11 M. N. Alvarez, G. Peluffo, L. Piacenza and R. Radi, *J. Biol. Chem.*, 2011, **286**, 6627.
- 12 A. T. Jacobs and L. J. Ignarro, *J. Biol. Chem.*, 2001, **276**, 47950.
- 13 W. H. Koppenol, J. J. Moreno, W. A. Pryor, H. Ischiropoulos and J. S. Beckman, *Chem. Res. Toxicol.*, 1992, **5**, 834.
- 14 S. V. Lyman and J. K. Hurst, *J. Am. Chem. Soc.*, 1995, **117**, 8867.
- 15 G. Merényi, J. Lind and S. Goldstein, *J. Am. Chem. Soc.*, 2002, **124**, 40.
- 16 G. Ferrer-Sueta and R. Radi, *ACS Chem. Biol.*, 2009, **4**, 161.
- 17 C. E. Donald, M. N. Hughes, J. M. Thompson and F. T. Bonner, *Inorg. Chem.*, 1986, **25**, 2676.
- 18 (a) K. M. Miranda, A. S. Dutton, L. A. Ridnour, C. A. Foreman, E. Ford, N. Paolocci, T. Katori, C. G. Tocchetti, D. Mancardi, D. D. Thomas, M. G. Espey, K. N. Houk, J. M. Fukuto and D. A. Wink, *J. Am. Chem. Soc.*, 2005, **127**, 722; (b) J. H. Jorolan, L. A. Buttitta, C. Cheah and K. M. Miranda, *Nitric Oxide*, 2015, **44**, 39.
- 19 R. Smulik, D. Debski, J. Zielonka, B. Michalowski, J. Adamus, A. Marcinek, B. Kalyanaraman and A. Sikora, *J. Biol. Chem.*, 2014, **289**, 35570–35581.
- 20 (a) H. Ischiropoulos, *Arch. Biochem. Biophys.*, 1998, **356**, 1; (b) R. Radi, *Proc. Natl. Acad. Sci. U. S. A.*, 2004, **101**, 4003.
- 21 (a) D. Yang, H. Wang, Z. Sun, N. Chung and J. Shen, *J. Am. Chem. Soc.*, 2006, **128**, 6004; (b) Z. Sun, H. Wang, F. Liu, Y. Chen, P. K. H. Tam and D. Yang, *Org. Lett.*, 2009, **11**, 1887.
- 22 (a) T. Peng, X. Chen, L. Gao, T. Zhang, W. Wang, J. Shen and D. Yang, *Chem. Sci.*, 2016, **7**, 5407; (b) J. Li, C. S. Lim, G. Kim, H. M. Kim and J. Yoon, *Anal. Chem.*, 2017, **89**, 8496.
- 23 X. Sun, Q. Xu, G. Kim, S. E. Flower, J. P. Lowe, J. Yoon, J. S. Fossey, X. Qian, S. D. Bull and T. D. James, *Chem. Sci.*, 2014, **5**, 3368.
- 24 F. Yu, P. Li, G. Li, G. Zhao, T. Chu and K. Han, *J. Am. Chem. Soc.*, 2011, **133**, 11030.
- 25 F. Yu, P. Li, B. Wang and K. Han, *J. Am. Chem. Soc.*, 2013, **135**, 7674.
- 26 Z. Lou, P. Li and K. Han, *Acc. Chem. Res.*, 2015, **48**, 1358–1368.
- 27 A. R. Lippert, *ACS Cent. Sci.*, 2017, **3**, 269.
- 28 W. Zhou, Y. Cao, D. Sui and C. Lu, *Anal. Chem.*, 2016, **88**, 2659–2665.
- 29 W. Zhou, S. Dong, Y. Lin and C. Lu, *Chem. Commun.*, 2017, **53**, 2122–2125.
- 30 T. S. Bailey and M. D. Pluth, *Methods Enzymol.*, 2015, **554**, 81.
- 31 L. Liu and R. P. Mason, *PLoS One*, 2010, **5**, e12024.
- 32 J. Cao, R. Lopez, J. M. Thacker, J. Y. Moon, C. Jiang, S. N. S. Morris, J. H. Bauer, P. Tao, R. P. Mason and A. R. Lippert, *Chem. Sci.*, 2015, **6**, 1979.
- 33 J. Cao, J. Campbell, L. Liu, R. P. Mason and A. R. Lippert, *Anal. Chem.*, 2016, **88**, 4995.
- 34 (a) O. Green, S. Gnaim, R. Blau, A. Eldar-Boock, R. Satchi-Fainaro and D. Shabat, *J. Am. Chem. Soc.*, 2017, **139**, 13243; (b) N. Hananya, A. E. Boock, C. R. Bauer, R. Satchi-Fainaro and D. Shabat, *J. Am. Chem. Soc.*, 2016, **138**, 13438.
- 35 A. P. Schaap, T. S. Chen, R. S. Handley, R. DeSilva and B. P. Giri, *Tetrahedron Lett.*, 1987, **28**, 1155.
- 36 O. Green, T. Eilon, N. Hananya, S. Gutkin, C. R. Bauer and D. Shabat, *ACS Cent. Sci.*, 2017, **3**, 349.
- 37 J. L. Kroll, C. A. Werchan, A. G. Reeves, K. J. Bruemmer, A. R. Lippert and T. Ritz, *Physiol. Behav.*, 2017, **179**, 99.
- 38 A. G. Reeves, M. Subbarao and A. R. Lippert, *Anal. Methods*, 2017, **9**, 3418.
- 39 M. E. Quimbar, K. M. Krenek and A. R. Lippert, *Methods*, 2016, **109**, 123.
- 40 K. J. Bruemmer, S. Merrikhagh, C. T. Lollar, S. N. S. Morris, J. H. Bauer and A. R. Lippert, *Chem. Commun.*, 2014, **50**, 12311.



41 T. Ueda, H. Konishi and K. Manabe, *Angew. Chem., Int. Ed.*, 2013, **52**, 8611.

42 J. M. Fukuto, M. D. Bartberger, A. S. Dutton, N. Paolocci, D. A. Wink and K. N. Houk, *Chem. Res. Toxicol.*, 2005, **18**, 790.

43 (a) K. Kawai, N. Ieda, K. Aizawa, T. Suzuki, N. Miyata and H. Nakagawa, *J. Am. Chem. Soc.*, 2013, **135**, 12690; (b) X. Jing, F. Yu and L. Chen, *Chem. Commun.*, 2014, **50**, 14253; (c) C. Liu, H. Wu, Z. Wang, C. Shao, B. Zhu and X. Zhang, *Chem. Commun.*, 2014, **50**, 6013; (d) K. Zheng, W. Lin, D. Cheng, H. Chen, Y. Liu and K. Liu, *Chem. Commun.*, 2015, **51**, 5754; (e) M. Ren, B. Deng, K. Zhou, J. Wang, X. Kong and W. Lin, *J. Mater. Chem. B*, 2017, **5**, 1954.

44 J. A. Reisz, C. N. Zink and S. B. King, *J. Am. Chem. Soc.*, 2011, **133**, 11675.

